Anterograde Tracing of the Rat Olivocerebellar System With Phaseolus Vulgaris Leucoagglutinin (PHA-L). Demonstration of Climbing Fiber Collateral Innervation of the Cerebellar Nuclei

J.J.L. VAN DER WANT, L. WIKLUND, M. GUEGAN, T. RUIGROK, AND J. VOOGD
Equipe de Neuroanatomie Fonctionnelle, Laboratoire de Physiologie Nerveuse, C.N.R.S.,
France (J.J.L.v.d.W., L.W., M.G.); Netherlands Ophthalmic Research Institute, Amsterdam
(J.J.L.v.d.W.), and Department of Anatomy, University of Rotterdam (T.R., J.V.), The
Netherlands

ABSTRACT

The olivocerebellar climbing fiber system was investigated in the rat with anterograde Phaseolus vulgaris leucoagglutinin (PHA-L) tracing. The specific objective of the study was to find morphological evidence of climbing fiber collaterals innervating the cerebellar nuclei.

Small iontophoretic injections of PHA-L were placed in different parts of the inferior olivary complex, and labelled olivocerebellar fibers could be traced to their termination as climbing fibers in sagittal zones of the contralateral cerebellar cortex. Reaching the cerebellum via the restiform body, the labelled olivocerebellar axons entered the deep cerebellar white matter anterior to the cerebellar nuclei. Most of these thicker, nonterminal axons continued dorsally around the nuclei, but some ran through them. Bundles of fibers could be followed into the folial white matter toward their cortical zones of termination.

Depending on which part of the olivary complex that was injected with PHA-L, labelled axons were seen to converge on different regions of the cerebellar nuclei, where dense plexuses of thin varicose terminal fibers appeared. Quantitative estimates of the innervation ranged from 1.7 to 4.3 million boutons per mm³ in the fastigial (FN), interposed, and main parts of the lateral cerebellar (LCN) nuclei, whereas the parvicellular portion of LCN demonstrated 15–20 million varicosities per mm³. Frequently, thicker olivocerebellar axons, which seemed directed toward the cerebellar cortex, were seen to send a fine collateral branch toward these areas of nuclear innervation.

As controls, PHA-L was injected into the degenerated olivary complex of 3-acetylpyridine-treated rats. Neither cortical climbing fiber terminals nor nerve terminal plexuses in the nuclei appeared in these experiments. In cases with injection sites extending into the reticular formation, substantial mossy fiber labelling was present bilaterally in the cortex, but the cerebellar nuclei were devoid of labelled innervation or demonstrated only a few larger diameter fibers.

The projection of the inferior olivary complex to the cerebellar nuclei was

strictly topographically organized and agreed in principle with the organization described in the cat by Groenewegen et al. ('79). The caudal medial accessory olive (MAO) projected to FN, the rostral MAO to the posterior interposed nucleus (NIP), the rostral part of the dorsal accessory olive (DAO) to the anterior interposed nucleus (NIA), and the principal olive (PO) to LCN. Smaller injections into olivary subnuclei resulted in labelled innervation in restricted sectors of individual cerebellar nuclei, suggesting the existence of a more detailed topographical organization.

Cerebellar climbing fibers originate in the contralateral inferior olive of the medulla oblongata (Eccles et al., '67; Desclin, '74) and synapse along the dendrites of the Purkinje cells (Cajal, '11; Palay and Chan-Palay, '74; Sotelo et al., '75). The topographical organization of the cat olivocerebellar projection has been investigated in detail, and it is generally accepted that specific compartments of the olivary subnuclei project to different sagittal zones of cerebellar cortex (for reviews: Brodal and Kawamura, '80; Voogd, '82). Recent investigations have shown that the organization of the rat olivocerebellar system follows similar principles (e.g., Campbell and Armstrong, '83a,b; Eisenman, '84; Wiklund et al., '84; Azizi and Woodward, '87). Moreover, the Purkinje cells in these sagittal zones project to distinct regions of the cerebellar nuclei (e.g., Voogd, '64; Dietrichs and Walberg, '80; Voogd and Bigaré, '80; Dietrichs, '81a,b; '83; Trott and Armstrong, '87a,b). In cats, the cerebellar nuclei also receive extracerebellar inputs through mossy fiber pathways originating in the spinal cord (Ikeda and Matsushita, '73) and certain (Künzle, '75; Russchen et al., '76; Gerrits and Voogd, '87; van der Want et al., '87) but not all (Dietrichs and Walberg, '87) brainstem nuclei projecting to the cerebellum.

In addition to their well-documented termination as climbing fibers in the cerebellar cortex, electrophysiological evidence has suggested that collaterals of the olivocerebellar axons innervate the cerebellar nuclei (Eccles et al., '74; Kitai et al., '77; Andersson and Oscarsson, '78); but the neuroanatomical evidence on this subject has remained controversial, and the existence of climbing fiber collateral innervation of the cerebellar nuclei has continued to be questioned. Electronmicroscopical investigations have revealed very few degenerating terminals in the cerebellar nuclei after olivary lesions (Angaut, '75; Desclin and Colin, '80). However, Chan-Palay ('73, '77) used ultrastructural similarities between terminals in the cerebellar nuclei and cortical climbing fibers as an argument for the existence of climbing fiber nuclear innervation. At the light microscopic level, several studies using degeneration techniques have concluded that an olivonuclear innervation exists (Matsushita and Ikeda, '70; Groenewegen and Voogd, '77; Balaban, '85). Retrograde tracing studies have generally indicated that an olivary input exists in all the cerebellar nuclei (Beitz, '76; Eller and Chan-Palay, '76; Kitai et al., '77; Dietrichs and Walberg, '85, '86, '87; Dietrichs et al., '85), but these types of investigation are hampered by risks of labelling passing fibers that do not terminate in the injected area. Some investigators using anterograde tracing with radioactive amino acids have reported an absence of (Courville '75) or only a sparse olivonuclear innervation (Courville and Faraco-Cantin, '78),

whereas other authors have interpreted their results as favouring the existence of a heavy innervation (Groenewegen and Voogd, '77; Groenewegen et al., '79). An investigation using selective labelling of climbing fibers with D-[³H]aspartate suggested the existence of an important collateral innervation of all cerebellar nuclei (Wiklund et al., '84). Finally, in the fastigial nucleus (FN), electron microscopic autoradiography has revealed labelling of axon terminals synapsing on dendrites after injection of [³H]leucine in the inferior olive of the cat (van der Want and Voogd, '87).

Gerfen and Sawchenko ('84) recently introduced PHA-L as an anterograde tracer that allows a very precise investigation of axonal projections; individual axons can be visualized from the site of injection toward terminal areas where terminal fibers with boutons and intervaricose segments appear in detail (Gerfen and Sawchenko, '84; Groenewegen and van Dijk, '84). In the present investigation, this technique was used to study the olivocerebellar system; the results demonstrate the existence of a topographically organized olivonuclear innervation and suggest that this innervation represents collaterals of climbing fibers projecting to the cerebellar cortex. A preliminary report of some of these findings has appeared (van der Want et al., '88).

MATERIALS AND METHODS

A total of 110 female and male Sprague-Dawley rats were used. Normal rats were of 220–280 g body weight. Forty rats (120–160 g) were treated with 3-acetylpyridine (3-AP) (Desclin and Escubi, '74; Llinas et al., '75) to induce degeneration of the olivocerebellar neurons: 75 mg/kg 3-AP (Fluka) intraperitoneally (i.p.), followed 3 hours later by 15 mg/kg harmaline-HCl (Sigma), and after another hour by 300 mg/kg niacinamide (Merck). Rats showing persistent motor disturbances after this treatment were used as controls in the PHA-L tracing experiments 3–8 weeks after the 3-AP treatment (when their weight had attained 200–260 g).

Surgical procedures and tracer application

Anaesthesia consisted of a mixture of ketamine (Imalgène®, Rhône Mérieux; 65 mg/kg) and xylazine (Rompun®, Bayer; 14 mg/kg), i.p.; small additional doses were given if the rats showed evidence of incomplete anaesthesia. Rats were placed in a Kopf stereotaxic frame. In most experiments (75 rats), a dorsal stereotaxic approach was used to reach the inferior olive with the micropipettes inclined 40° caudally to avoid penetrating the cerebellum. In other cases, a ventral approach was used with direct visual control through the operation microscope. These rats were mounted upside-down, skin incised, and the trachea pulled laterally,

giving access to the base of the skull. The musculature covering the base of the cranium was removed bluntly, a hole drilled in the bone, and the dura incised to expose the ventral surface of the brainstem. The basilar artery, pyramid, and the foramen magnum were used as landmarks to localize the inferior olive.

Glass micropipettes with 18–24 μm inner tip diameters were filled with 2.5% PHA-L in 0.1 M sodium phosphate buffer, pH 7.4 or 8.0. The tracer was injected iontophoretically by using a positive current of 5–8 μA, pulsed 5 seconds on and 5 seconds off, for a total of 10–20 minutes. Pipettes were left in situ for an additional 5 minutes before withdrawal, and sulfanilamide (Exoseptoplix®, Théraplix, France) was applied to the wound before suturing.

Fixation and immunohistochemistry

Modifications of previously published methods were used (Gerfen and Sawchenko, '84; Wouterlood and Groenewegen, '85). After 5–12 days survival, rats were reanaesthetized with chloral hydrate and fixed by perfusion through the ascending aorta. Blood was rinsed out with a chilled solution containing 0.8% NaCl, 0.8% sucrose, and 0.4% d-glucose in 0.05 M phosphate buffer (pH 7.4, approximately 200 ml), followed by 500 ml fixative consisting of 0.5% paraformaldehyde, 2.5% glutaraldehyde, and 4.0% sucrose in the same buffer delivered over 20–30 minutes. Dissected brains were kept in the same fixative overnight at 4°C and transferred to 30% sucrose in phosphate buffer, where they were kept until they sank.

Blocks of the lower medulla oblongata containing the inferior olive were cut transversely at 30 μm, and the cerebellum and upper brainstem were cut sagittally or transversely at 30 μm (or 20 μm) on a freezing microtome. Serial sections were collected in perspex containers with Tris buffered saline (TBS) (0.9% NaCl in 0.05 M Tris-HCl, pH 7.4) for immunocytochemical treatment of serial sections. Sections were rinsed three times for 15 minutes in TBS, free aldehyde groups reduced by 1% sodium borohydride in TBS for 30 minutes, rinsed three times again for 15 minutes, endogenous peroxidase activity quenched by 0.3% H$_2$O$_2$ in methanol for 30 minutes, and rinsed another three times for 15 minutes in TBS containing Triton X100 (TBS-T) (0.05 M NaCl, 0.2–0.4% Triton X100, in 0.05 M Tris-HCl, pH 8.6). Sections of the lower medulla were usually incubated 16–18 hours in the primary antiserum at room temperature for rapid evaluation of injection sites, whereas cerebellar sections were incubated for 3–5 days at 4°C in goat anti-PHA-L serum (Vector), 1/2,000 in TBS-T containing 2% normal rabbit serum. As controls, some sections were incubated without primary antiserum. Subsequently, sections were rinsed 3 times for 15 minutes in TBS-T, incubated for 2 hours in rabbit antigoat globuline serum (ICM, Sweden) at 1/200 in TBS-T containing 2% rabbit normal serum, rinsed three times 15 minutes in TBS-T, incubated for 2 hours in goat-PAP (ICM) at 1/400 in TBS-T, and rinsed for three times for 15 minutes in Tris-HCl (0.05 M, pH 7.6) before diaminobenzidine (DAB) processing. In early experiments, sections were incubated in 0.05% DAB (3,3'-diaminobenzide-tetrahydrochloride, Sigma) and 0.01% H$_2$O$_2$ in Tris-HCl for 10–30 minutes. Later experiments used a modification of the cobalt-glucose oxidase method (Itoh et al., '79): sections were preincubated for 10 minutes in 0.5% cobalt acetate in Tris-HCl, rinsed in Tris-HCl for 15 minutes followed by two 15 minutes washes in 0.1 M phosphate buffer (pH 7.3), and incubated for 20–60 minutes in a solution con-

taining 0.05% DAB, 0.2% β-D-glucose (Sigma) and 0.4% ammonium chloride (Sigma) in phosphate buffer, and glucose oxidase (Merck) (0.3 mg/100 ml), which was added immediately before starting incubation. Reacted sections were rinsed three times in phosphate buffer for 15 minutes, mounted onto chrome alum-gelatinized slides, air-dried, sometimes counterstained with cresyl violet or thionine, and coverslipped with Distrene-80 (Gurr).

Microscopic evaluation

Results were evaluated by brightfield (with a Kodak Wratten no. 46 blue filter), Nomarski interference contrast, and darkfield microscopy using a camera lucida. Subdivisions of the inferior olivary complex were identified according to published descriptions (Gwyn et al., '77; Wiklund et al., '84; Azizi and Woodward, '87), and Korneliussen ('68) and Voogd et al. ('85) were consulted for delineation of cerebellar nuclei.

Terminal density was estimated in selected cases. A chosen sector of neuropil was viewed under 100× oil immersion objective while systematically focusing through the depth of the tissue section. The position of labelled varicosities was recorded with the camera lucida on a white sheet of paper. A micrometer slide was used to calibrate the actual magnification of the resulting drawing, and the number of varicosities was counted and divided by the calculated volume of investigated tissue. Previous estimates showed that shrinkage of tissue during fixation was virtually compensated for by swelling during the subsequent immunocytochemical procedure, and no "shrinkage factor" was therefore included in the calculations.

RESULTS
Injection sites

The PHA-L injection sites were usually characterized by a diffuse immunostaining in which individual labelled perikarya sometimes could be observed. Less frequently, injection sites were characterized by an accumulation of immunostained olivary cell bodies, as has been described in previous investigations using this tracer (Gerfen and Sawchenko, '84; Wouterlood and Groenewegen, '85). These differences in appearance of the injection sites did not seem to influence the anterograde tracing. In most cases, the site of injection was easily defined, and labelled parts of the olivary complex were clearly distinguishable from neighbouring tis-
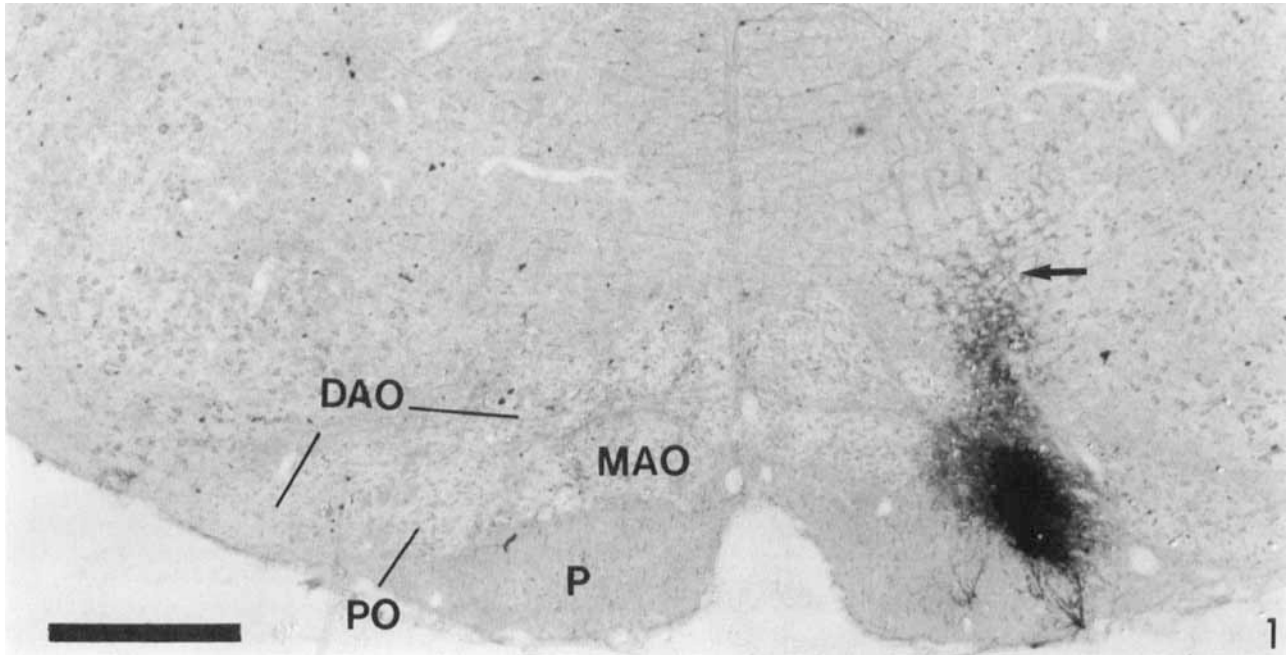
Fig. 1. PHA-L injection site centered on the caudal PO (level 8, Fig. 12). A dorsal stereotaxic approach was used in this experiment, and some leakage of tracer occurred along the tract of the micropipette (arrow). Bar = 250 µm.
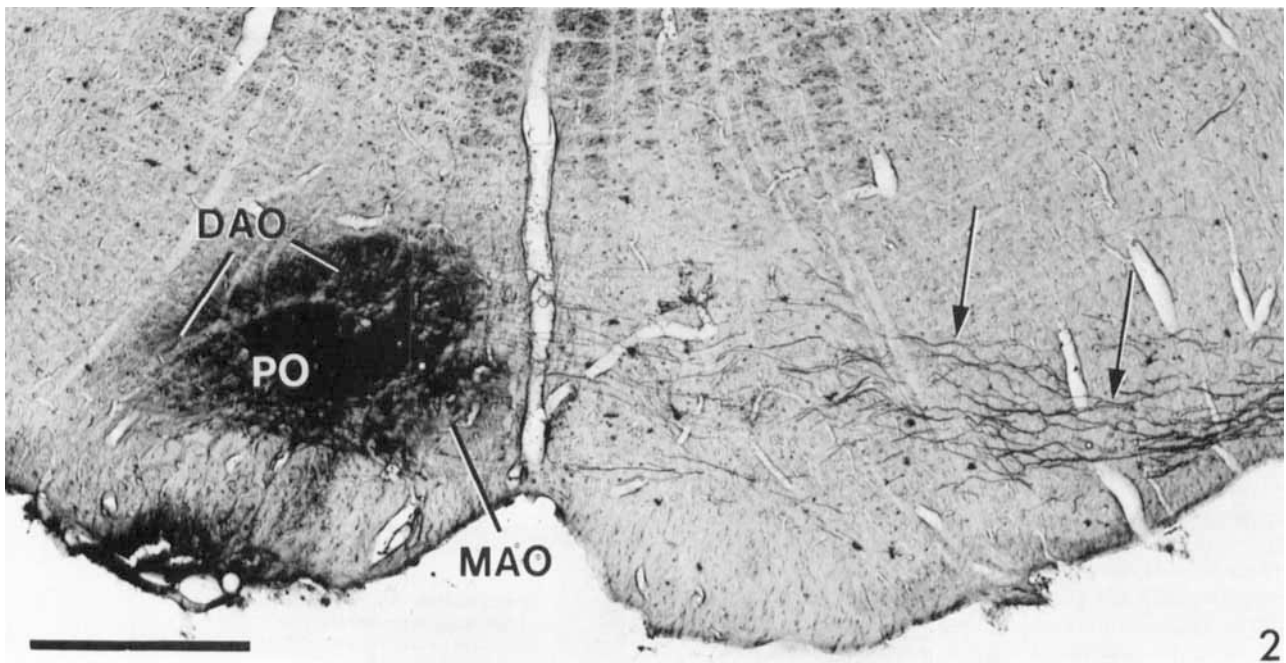

Fig. 2. PHA-L injection site in a case where a ventral surgical approach was used. Injection at level 13 (see Fig. 12) involving parts of PO, DAO, and rostral MAO. Note the anterograde labelling of axons along the olivocerebellar tract (arrows) on the contralateral side. Bar = 250 µm.

sue. The sizes of injection sites varied considerably from small injections of a portion of a subnucleus (Fig. 1) to injections covering a large part of the olivary cross section (Fig. 2).

Distant perikarya outside the limits of the injection site were sometimes labelled. The contralateral olive sometimes demonstrated a small number of well-stained neurons with their axon directed toward the center of the injections site (Fig. 3). It seemed likely that these represented retrograde labelling of neurons whose axon had been lesioned by the
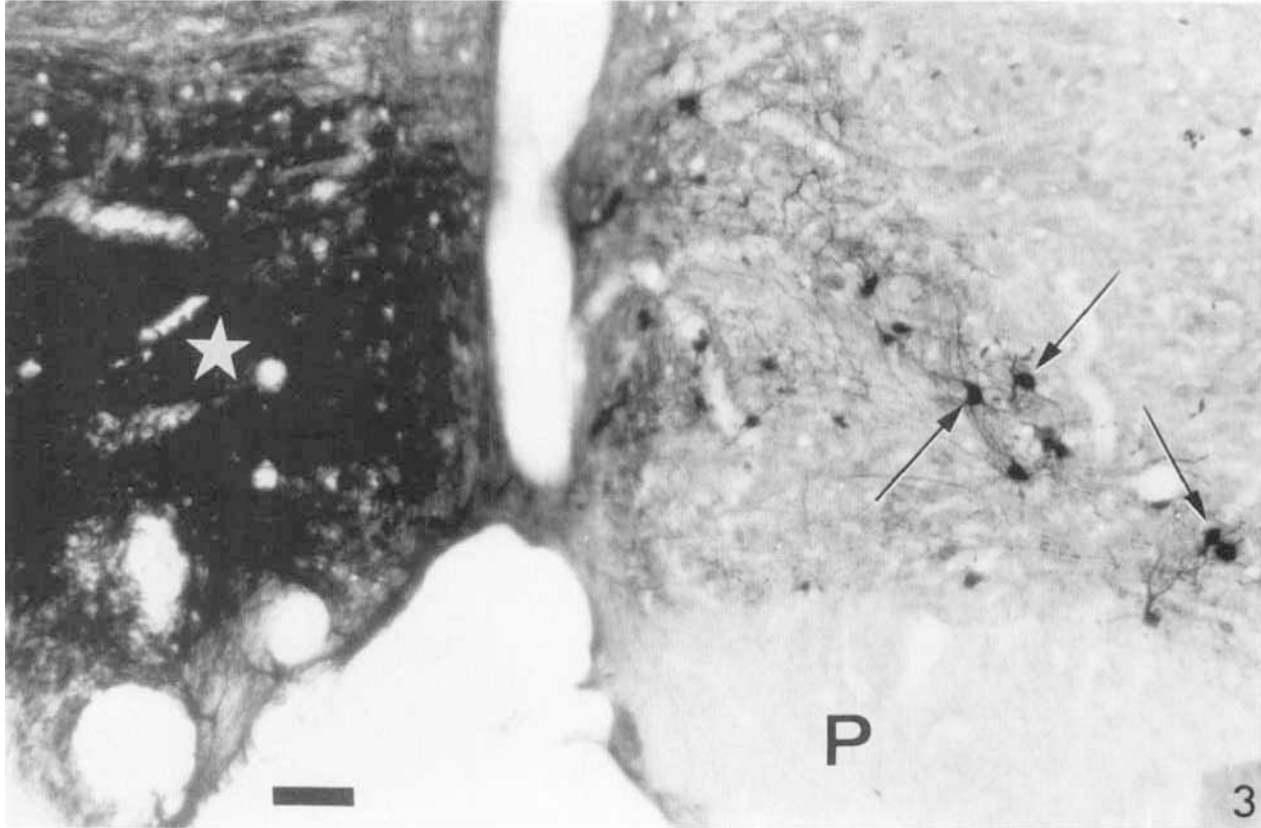
Fig. 3. Micrograph of an injection site to examplify the phenomenon of retrograde PHA-L labelling encountered in some experiments. A dense injection site is visible in the left MAO (white star), but it does not directly involve the contralateral MAO. However, this nucleus displays a number of well-stained neurons (arrows), and because the axons of these MAO cells are known to pass through the injected area, it is suggested that they may represent retrogradely labelled cells whose axons may have been lesioned by the iontophoretic injection.

iontophoretic PHA-L injection (Wiklund et al., 1984). Similarly, labelled reticular neurons could sometimes be observed at a distance from the injection site.

Immunolabelling was sometimes observed along the micropipette tract (Fig. 1), but it did not always seem to have resulted in appreciable anterograde labelling. In experiments in which the ventral surgical approach had been used, some cases had to be discarded because the injections were located dorsally or ventrally to the olivary complex. Representative cases with injections in different parts of the inferior olive were selected for detailed analysis.

Olivocerebellar tracing

From injection sites, axons could be followed across the midline, traversing the medulla oblongata to join the restiform body along the olivocerebellar trajectories already described (Wiklund et al., '84). Depending on the part of the olive injected, labelled fibers ran dorsally before crossing the midline and passing above the contralateral olive, whereas other axons crossed more ventrally to traverse or pass ventral to the contralateral olive.

Labelled axons in the restiform bodies were 1–2 μm in diameter and displayed spindle-shaped swellings (2–4 μm) along their course (Figs. 4, 5). Since fibers in the cerebellar white matter were of similar character (Figs. 5, 6, 8, 11), this type of fiber was considered as typical for the non-terminal parts of olivocerebellar axons.

Sagittal sections gave the most informative view of the olivocerebellar axons reaching the cerebellum. The labelled fibers arriving through the restiform body reached the cerebellar white matter rostral to the cerebellar nuclei (Figs. 5, 13). Most fibers ran dorsally and caudally in the white matter immediately around the deep nuclei, but some axons traversed the nuclear neuropil. Fibers from different parts of the olivary complex occupied different mediolateral positions in the white matter: fibers from the caudal medial accessory nucleus (MAO) running medially around the FN (Fig. 15); fibers from rostral MAO and the dorsal accessory nucleus (DAO) over and through the interposed nuclei (Figs. 5, 13); and fibers from the principal olivary nucleus (PO) around the lateral cerebellar nucleus (LCN) (Figs. 6, 14). Bundles of fibers left the deep cerebellar white matter to form bundles running into different folia (Figs. 5, 13–15). On frontal sections, these appeared as sagittally oriented bundles, and in the molecular layer of overlying cortex typical climbing fiber terminals appeared in distinct sagittal zones (Figs. 14, 15).

Branching olivocerebellar axons were sometimes seen in the cerebellar white matter rostral to the deep nuclei. At these branching points, both collaterals were of the thicker nonterminal character and therefore might represent the well-known climbing fiber collateralizations projecting toward different parts of the cerebellar cortex (Armstrong et al., '73a,b; Brodal et al., '80; Rosina and Provini, '83; Wiklund et al., '84).

Fig. 4. Brightfield view of labelled olivocerebellar axons in the resti-
form body close to its entering the cerebellar white matter. Note the
slightly contorted course of these axons, and that they display spindle
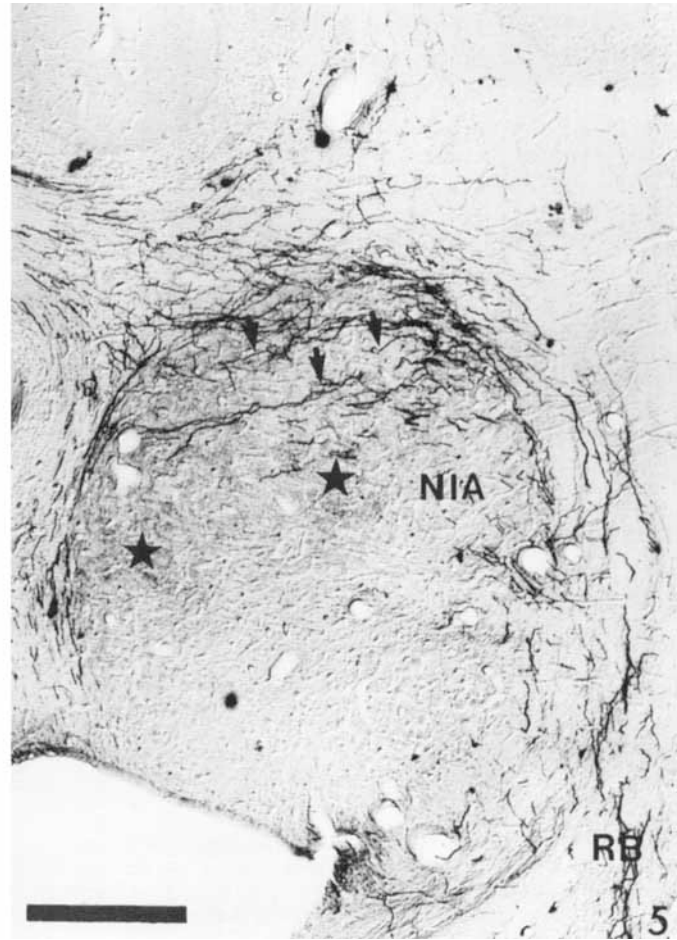shaped swellings at irregular intervals. Bar = 10 µm.

Fig. 5. A low-power micrograph of a sagittal section through part of
the cerebellar nuclei and deep white matter, as seen in Nomarski optics.
This rat had received a PHA-L injection into the rostral MAO, and

labelled olivocerebellar axons are seen arriving via the restiform body
rostral to the deep nuclei. Most fibers form a bundle in the white matter
just dorsal to the nuclei, but a considerable number traverse NIA. These
traversing fibers (arrows), as well as fibers arriving from dorsal, seem to
converge on areas of terminal innervation in NIP (stars). (The plexus of
fine terminal fibers is hardly visible at this low magnification, but it
results in a deeper gray shade of immunoreactivity.) Note also the bun-
dles of olivocerebellar axons which continue into folial white matter.
Bar = 250 µm.

In the cerebellar cortex, the labelled climbing fiber arbo-
rizations (Figs. 7a,b) demonstrated their distinct morpho-
logical characteristics, which are well known from Golgi
studies (Palay and Chan-Palay, 1974). Sagittal sections tend
to show the climbing fibers "en face." Axons could be traced
up through the granular layer toward a Purkinje cell body
on which some tortuous bends of fiber were formed. A
thicker main axon stem ascended the molecular layer and
gave rise to numerous thinner varicose fibers. In the granu-
lar layer, fine tendrils branched off the arriving climbing
fiber and could be traced for different distances. Frontal
sections showed the climbing fiber terminal "en profile,"
and they appeared as rows of terminals surrounding Pur-
kinje cell dendritic trees (Fig. 7a).

Surprisingly, Purkinje cells receiving especially well-
labelled climbing fibers often showed a weak immunolabel-
ling, suggesting a transcellular transfer of PHA-L (Fig. 7b).
Moreover, transfer of tracer from passing axons to glia

seemed sometimes to occur in the white matter. This phe-
nomenon was encountered within intensely labelled bundles
of fibers, e.g., in the restiform body and the parafascicular
peduncle, as scattered cells of astroglial character demon-
strating a strong immunolabelling.

Labelled fibers in the cerebellar nuclei

The cerebellar nuclei were subject to detailed investiga-
tion. Circumscribed areas of their neuropil demonstrated
rather dense plexuses of fine varicose fibers, which were
interpreted as terminal innervation (Figs. 8, 9). The diame-
ter of their intervaricose segments was estimated at 0.4–0.5
µm; varicosities measured 1–1.4 µm. The morphology of
these thin varicose fibers was distinct from that of nonter-
minal olivocerebellar axons, but it was reminiscent of the
fine varicose branchlets of climbing fiber terminals in the
molecular layer. Labelling of these fine fibers was never
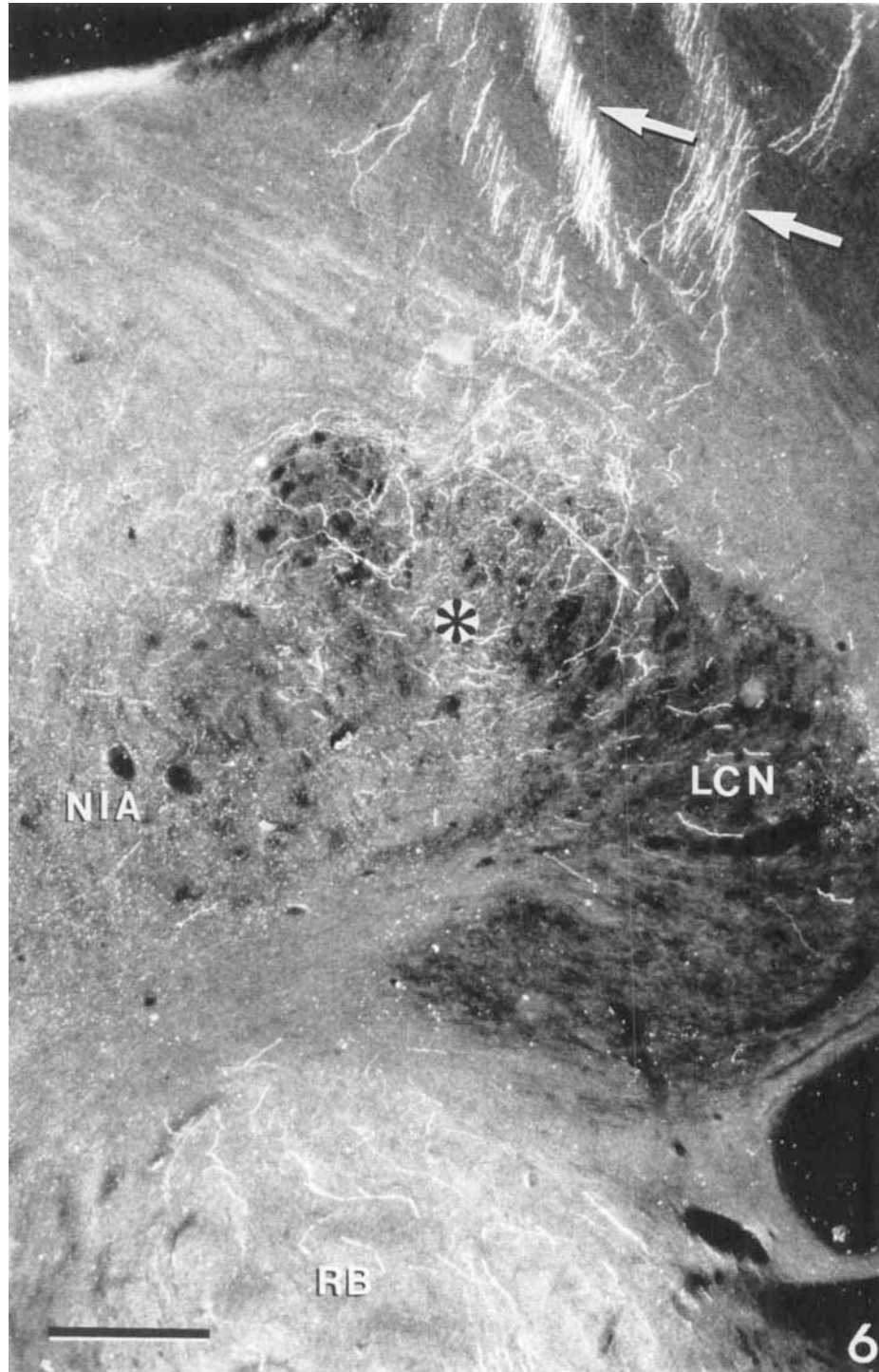intense. Sometimes only the varicosities seemed to contain

Fig. 6. Darkfield micrograph of a frontal section through the deep cerebellar white matter and nuclei of an experiment with a PHA-L injection into part of PO and rostral DAO. Labelled axons can be seen in the restiform body (lower part of picture). Bundles of labelled axons directed toward the cerebellar hemispheres (arrows) seem continuous with innervated areas of the LCN (asterisk) and the NIA. At this low magnification, the plexuses of nerve terminals in the nuclei appear as "clouds" of fine dots representing individual varicosities. In the lateral cerebellar nucleus, the sector receiving labelled terminals is sharply demarcated from neighbouring tissue that does not receive labelled innervation, suggesting a detailed topographical organization of the PO projection to the lateral cerebellar nucleus. Bar = 250 μm.
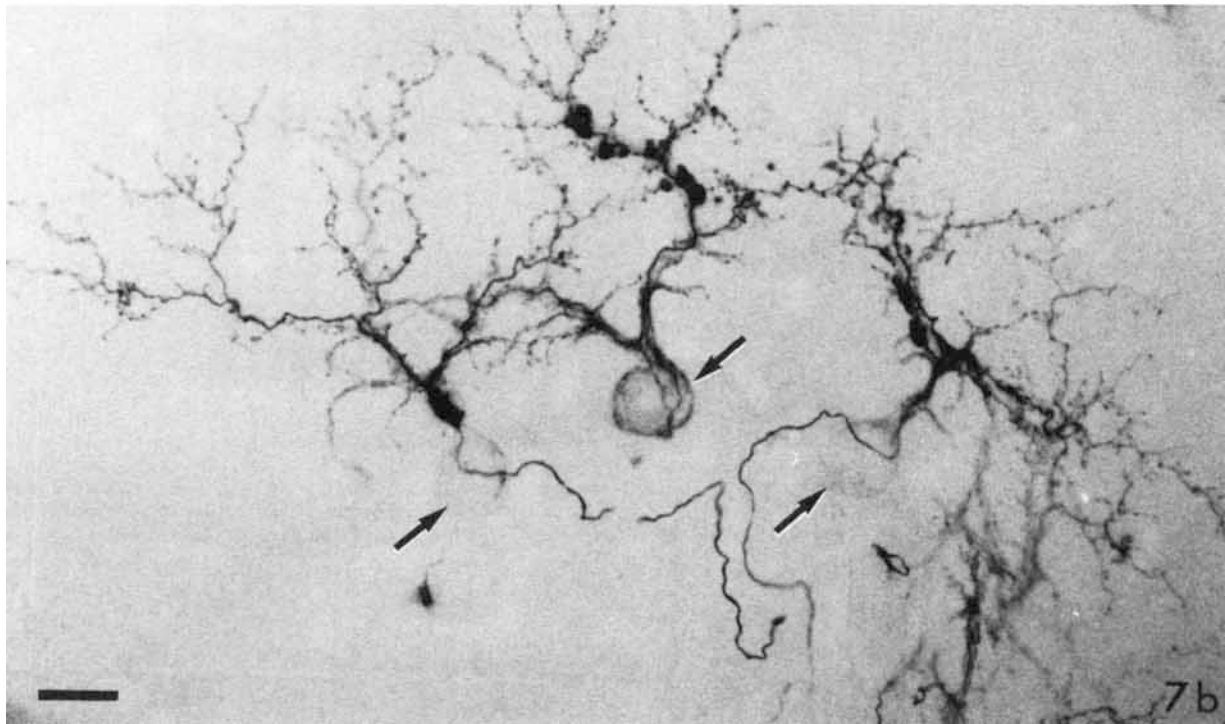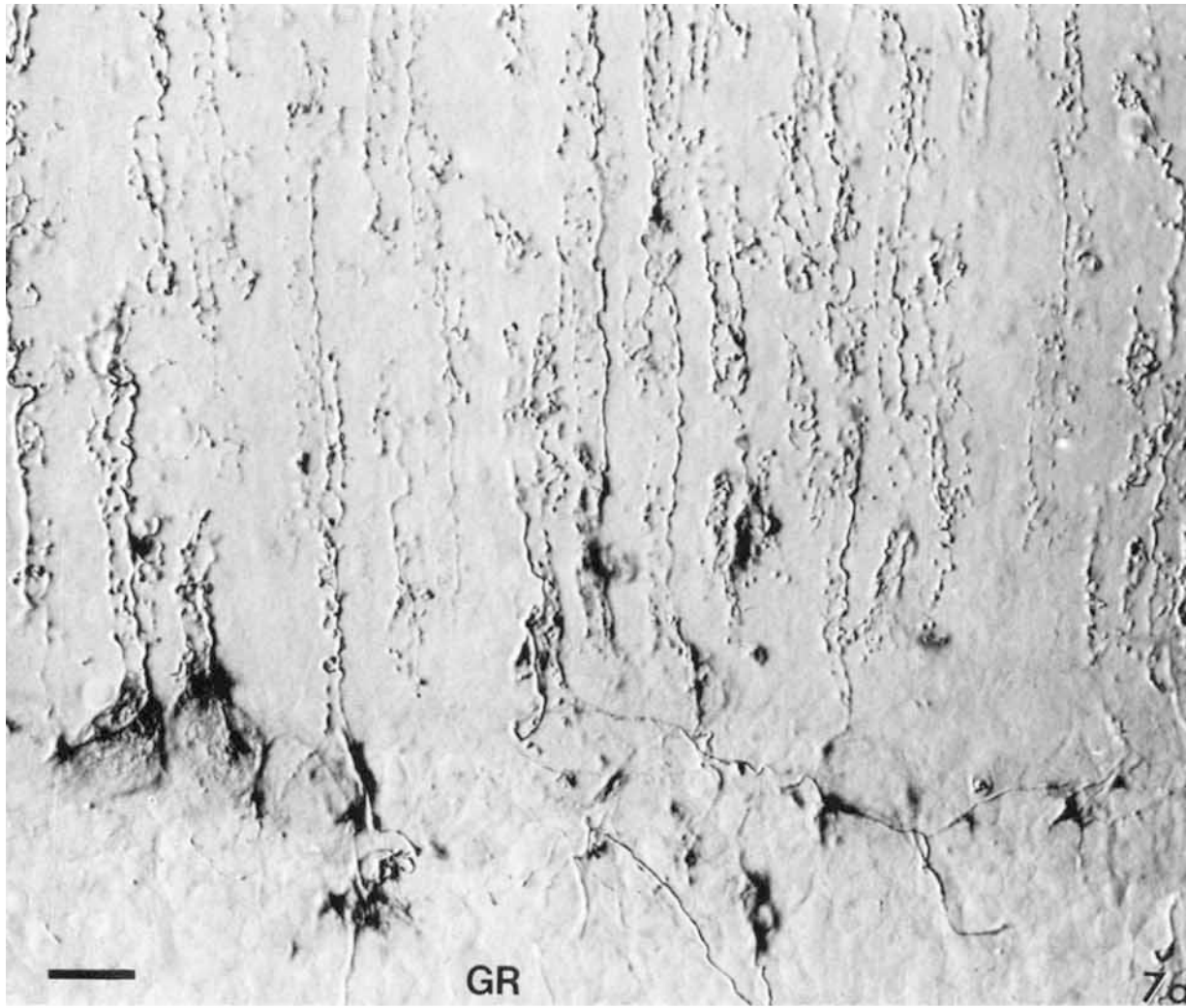
GR

7b

7b

Figure 7

detectable levels of immunoreactivity or the intervaricose segments were barely visible, giving the innervation plexus an appearance of a cloud of punctate immunoreactivity.

Olivocerebellar axons converged onto these plexuses of fine terminal fibers (Figs. 5, 6, 8, 13–15). Moreover, these thicker axons were on several occasions seen to send fine collateral branches toward these areas of innervation. A particularly illustrative example is shown in Figure 11. On this photomontage, a thick olivary axon running in the white matter border of the LCN gives off a fine-diameter collateral branch, which can be traced for about 160 μm into the underlying neuropil. Especially the distal part of the visualized thin collateral displays varicose swellings, suggesting formation of synaptic contacts. A reasonable interpretation is that the fine collateral contributes to the innervation of the LCN, whereas the main axon continues toward the cerebellar cortex, where it will terminate as a climbing fiber. Olivocerebellar axons traversing the deep nuclei were also observed sending collaterals to innervated areas of the neuropil (Fig. 10).

Topography of olivonuclear innervation

To illustrate the topographic organization of different olivary compartments projecting to distinct parts of the deep cerebellar nuclei, some of our cases will be described. A schematic illustration of the olivary complex as seen on 15 equidistant frontal sections is given by Figure 12. In the descriptions of individual cases, injection sites will be characterized in reference to these levels.

The results of experiment 40 are illustrated by Figure 13. This PHA-L injection was centered on the rostral MAO, but the tracer had also spread into the ventral lamella of PO. The cerebellum and upper brainstem were sectioned sagittally. Labelled axons could be traced through the restiform body into the deep cerebellar white matter. Many fibers continued dorsally and caudally around the deep nuclei, but a considerable number of axons traversed the anterior interposed nucleus (NIA) and other parts of the deep nuclei. In the posterior interposed nucleus (NIP), areas of dense nerve terminal labelling appeared. Olivary axons arriving from dorsal as well as fibers traversing the NIA seemed to contribute to the innervation of NIP. It seems likely that the innervation of NIP originated in rostral MAO, whereas the less conspicious aggregations of terminals observed in LCN (Fig. 13, level 1) originated in PO (see below).

In experiment 77, the PHA-L injection was completely restricted to rostral MAO, and a rich innervation of NIP was noted on frontal sections of the cerebellum. Experiment 62 demonstrated a small injection restricted to PO, and labelled terminals could be detected in a portion of LCN.

Case 49, illustrated by Figures 6 and 14, demonstrated a large PHA-L injection covering the rostral levels of PO and part of the overlying DAO. The sagittal organization of the cortical climbing fiber innervation was obvious on the frontal cerebellar sections. Axons converge on LCN, where a densely innervated sector appears, and on NIA, where a less dense plexus of terminals was located. Comparison with

other cases suggest that innervation of LCN originates in PO, whereas DAO projects to NIA.

The PHA-L injection in rat 81 (Fig. 15) centered on the caudal MAO but continued into the transition zone of MAO (Azizi and Woodward, '87). A rich plexus of labelled terminals was located in two sectors of FN and presumably originated in caudal MAO. A smaller plexus of innervation was observed in neighbouring parts of medial NIP. Several experiments (data not shown) demonstrated PHA-L injections involving other parts of caudal MAO and labelled nerve terminals in other sectors of FN.

Quantification of labelled terminals

Subjectively, the terminal innervation demonstrated in different cerebellar nuclei was rather dense and seemed to vary in different regions of the deep nuclei. In a few cases, we counted the number of labelled varicosities, probable sites of synaptic interactions, in the center of the innervated sectors.

Rat number 40 had an injection centered on rostral MAO, and the number of varicosities in the densely innervated NIP was estimated to 1.7×10^6 per mm^3. Rats number 49 and 39 had PHA-L injections centered on PO, and the density of varicosities in the innervated areas of the LCN were estimated to 3.4×10^6 and 4.3×10^6 per mm^3, respectively. Rat 51 had an injection covering central PO, as well as rostral MAO and DAO, and a count in the most densely labelled area of the interposed nuclei gave an estimate of 1.7 million per mm^3. Rat 52 with a PHA-L injection in caudal MAO demonstrated a densely innervated area in the center of the fastigial nucleus, with an estimated number of 2.6 million varicosities per mm^3. Rats 69, 71, and 76 were injected with PHA-L in the medial parts of caudal MAO, i.e., covering the ventrolateral outgrowth and dorsal cap, and demonstrated very high densities of labelled terminals in the parvocellular part of LCN; estimates ranged between 15 and 20 million varicosities per mm^3

Mossy fiber labelling

Some rats injected with PHA-L into the olivary complex were completely devoid of mossy fiber labelling, although the cortex showed large numbers of climbing fiber terminals. Other cases showed bilaterally a varying number of mossy fiber endings in different parts of the cerebellar cortex. Mossy fiber labelling was more abundant when the PHA-L injection site spread into the reticular formation outside the olive.

3-acetylpyridine treated cases

A number of cases with efficient 3-AP-lesioning of the inferior olive were analyzed. Cresyl violet stained sections revealed a shrunken olivary complex dominated by glial cells and where all, or almost all, neuronal perikarya had disappeared. PHA-L injections placed into the 3-AP lesioned olive were less distinct than in normal animals, indicating that the lack of neurons decreased the retention of the applied tracer.

The 3-AP pretreatment resulted in a marked decrease or a complete lack of climbing fiber labelling in the cerebellar cortex, and the cerebellar nuclei were devoid of terminal plexuses of fine varicose fibers. For example, in a particularly successful case (3AP 9), three PHA-L injections were restricted to the olivary complex (rostral and caudal MAO, ventral PO) and the underlying pyramid. A few PHA-L-stained cells of reticular formation character were seen

---

Fig. 7. **a:** Nomarski interference micrograph of well-labelled climbing fiber terminals ("en profil") in the molecular layer. **b:** Very well-stained climbing fiber terminals seen "en face" on a sagittal section. Note the immunoreactivity of the Purkinje cell bodies (arrows), suggesting a transcellular (or transsynaptic) transfer of PHA-L from the climbing fibers. Bars = 15 μm.
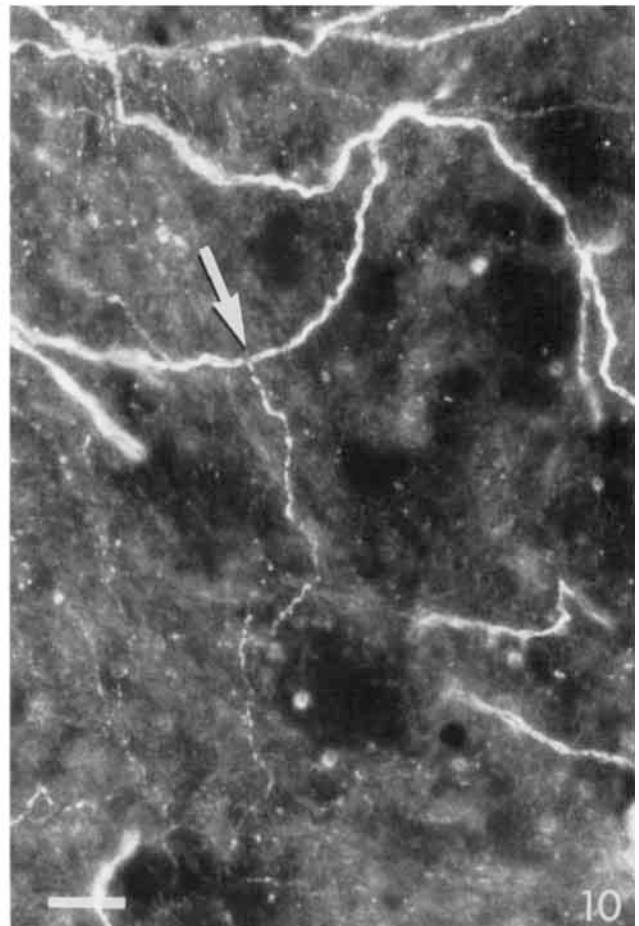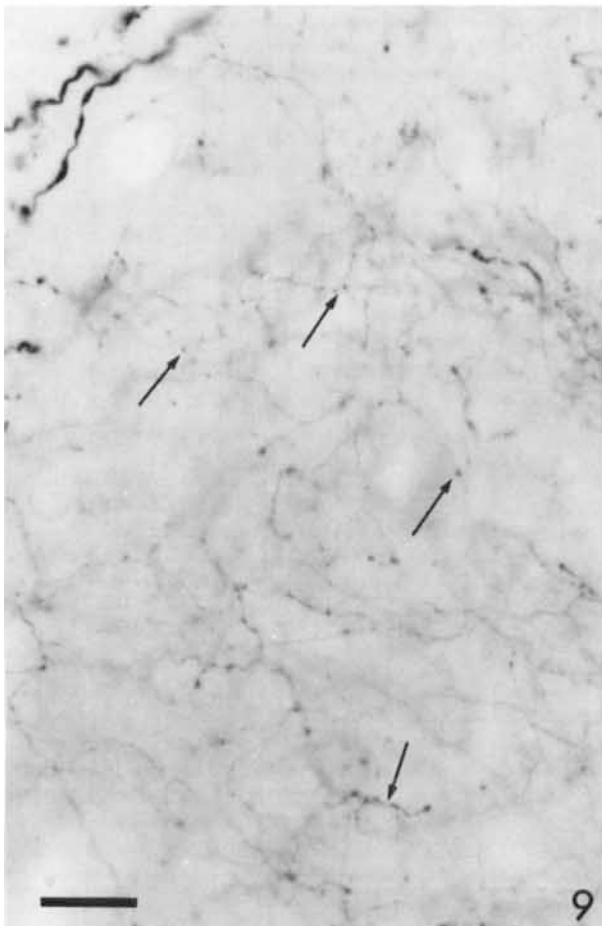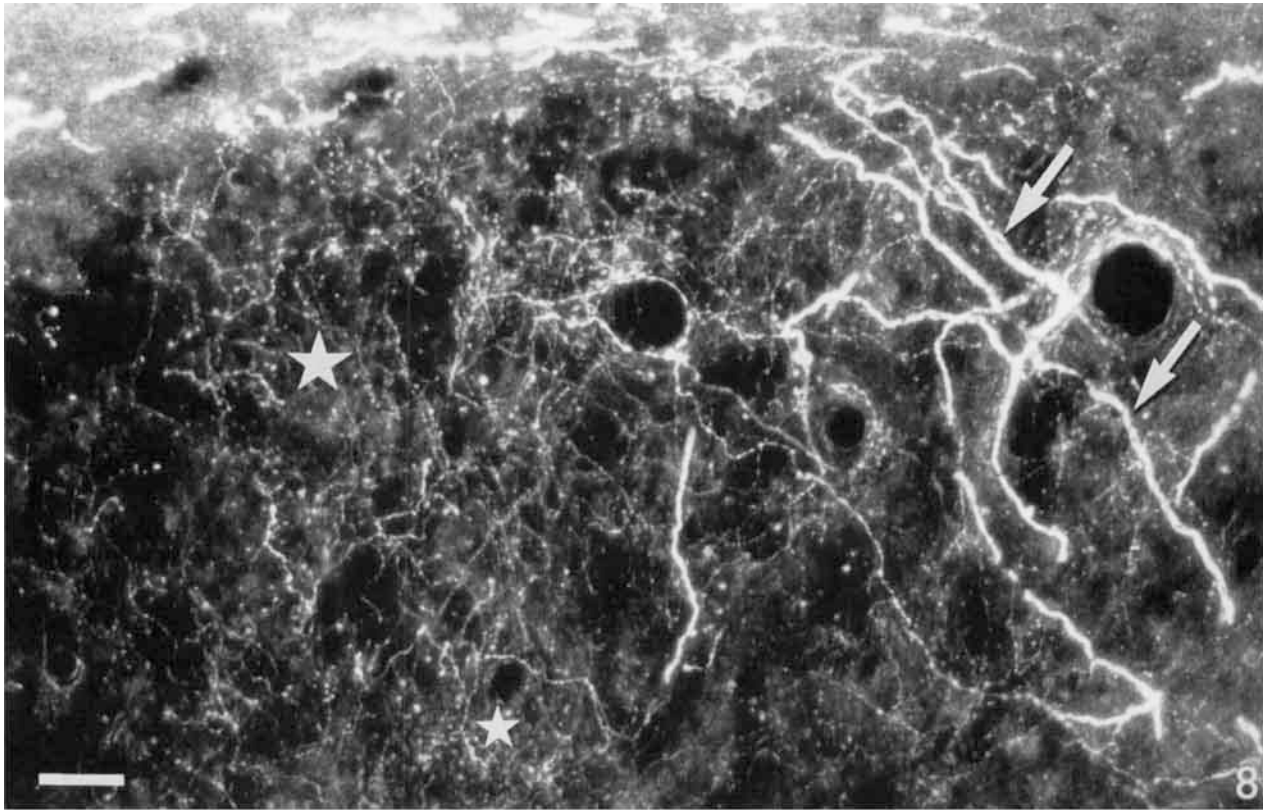
Figures 8–10
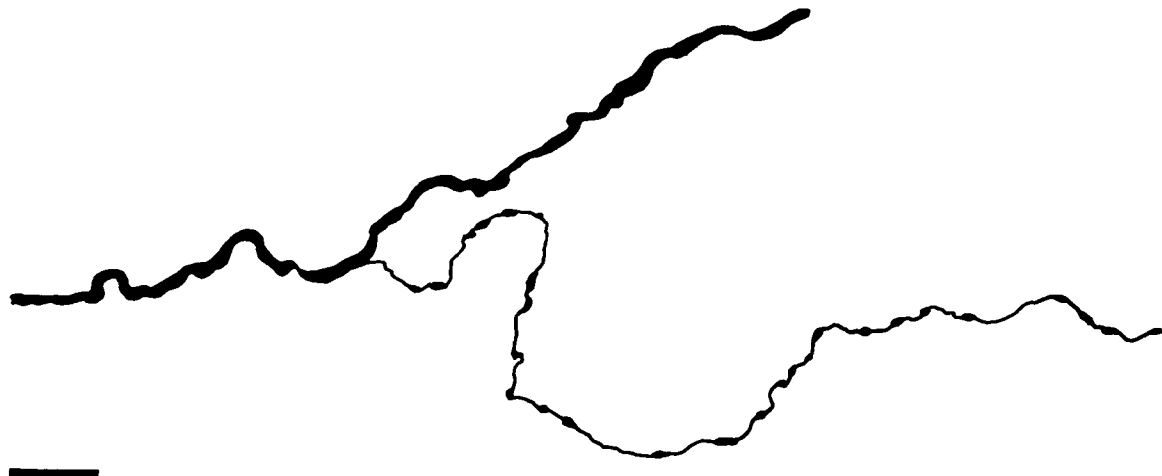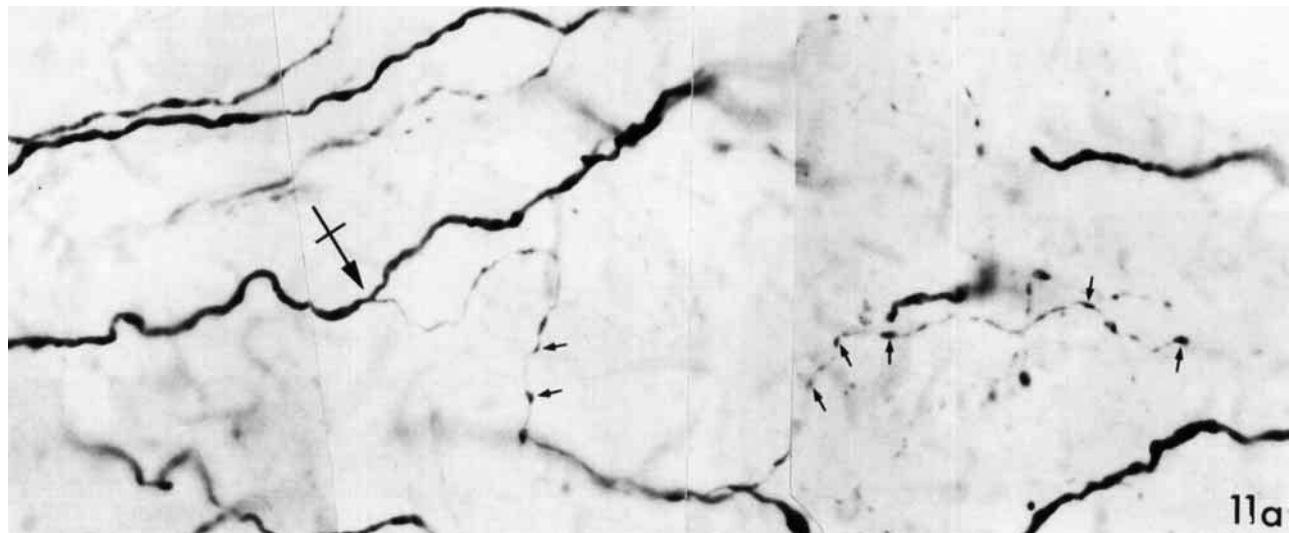
Fig. 11. Olivary axon in the border of the white matter and interposed nuclei, which gives off a thin collateral toward an area of innervation. a: Photomontage of pictures taken under oil immersion. The branching point is indicated by a crossed arrow. The thin collateral follows a tortous course (for a short distance it is obscured by an underlying thicker axon) and demonstrates several varicosities that may be the sites of synaptic interaction (small arrows). b: Schematic drawing of the same fiber. Bar = 20 μm.

Fig. 8. Darkfield micrograph of a sector of the LCN in a sagittally sectioned specimen. Thicker olivocerebellar axons (larger arrows) run in the overlying white matter and some traverse the neuropil in the right part of the micrograph. These arriving olivary axons seem to give rise to the dense plexus of thin varicose terminal fibers (stars), which extend over most of the illustrated neuropil. Bar = 20 μm.

Fig. 9. Brightfield micrograph of olivary terminals in the LCN at high magnification. Note the extremely fine character of these terminal fibers (examples indicated by fine arrows); the intervaricose segments are barely visible, whereas the frequent varicosities contain more immunoreactive material. Some thicker olivocerebellar axons of nonterminal character are seen in the upper left corner. Bar = 20 μm.

Fig. 10. Darkfield micrograph of thicker olivocerebellar axons giving off a fine varicose collateral toward a nuclear area containing labelled innervation. Arrow indicates branching point. Bar = 20 μm.

between the lamellae of the degenerated olive, and a small number of fibers could be identified in medullary and pontine tegmentum. However, the cerebellar cortex and deep nuclei were completely devoid of labelled fibers.

Certain cases showed PHA-L injections extending into the neighbouring reticular formation. In these experiments, a few labelled fibers could be found ipsilaterally or contralaterally in the cerebellum; the deep cerebellar white matter showed occasional coarser fibers, and the cerebellar cortex demonstrated a number of mossy fiber endings. Occasionally, some coarser fibers ran into the cerebellar nuclei, but in only one case did a fiber seem to terminate with a few large diameter varicosities in the interposed nuclei ipsilateral to the injection.
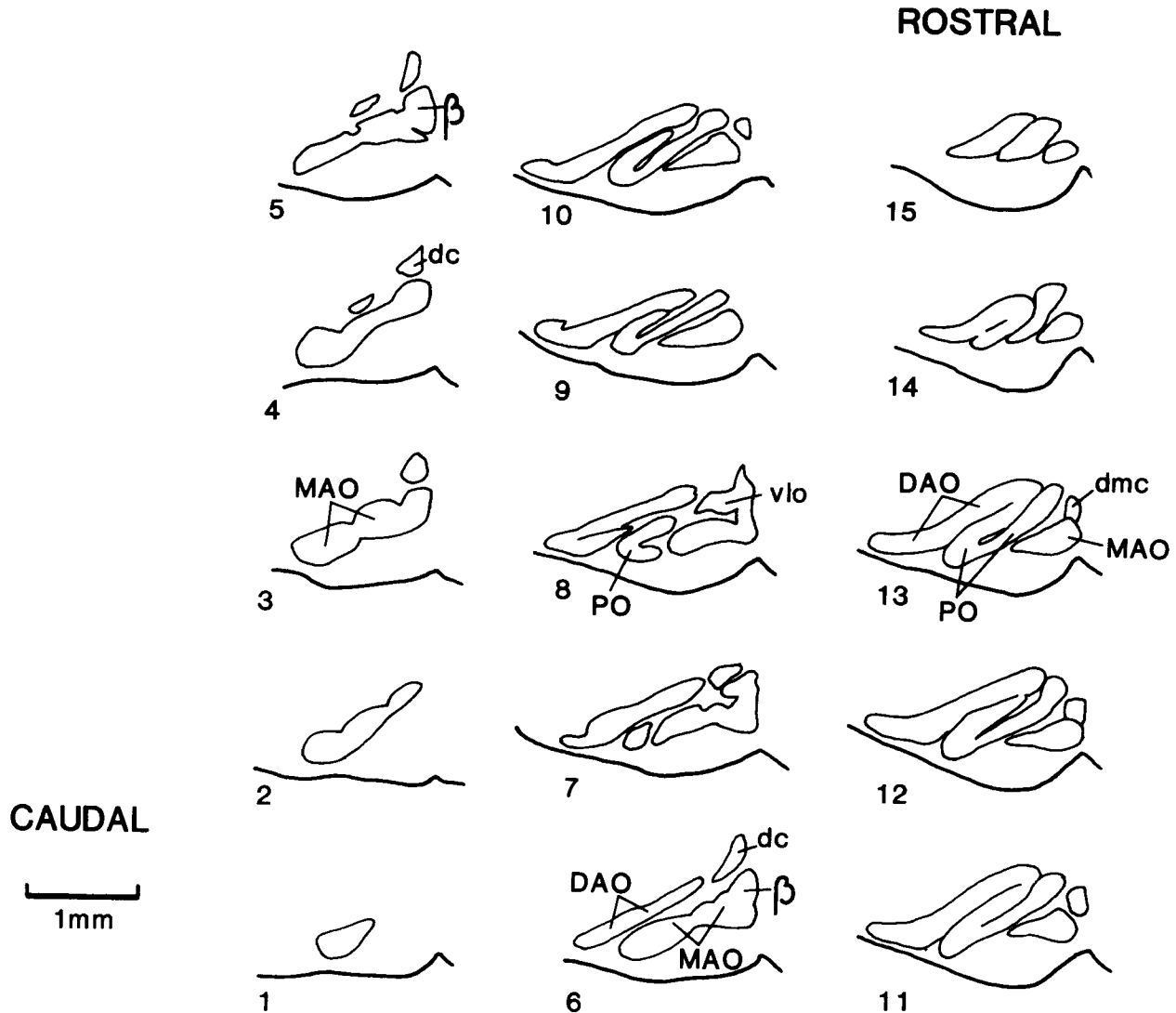
ROSTRAL

Fig. 12.   Schematic drawing of the olivary complex as it appears on 15 approximately equidistant rostro-caudal levels. Illustrations of individual experiments (Figs. 1, 2, 13–15) refer to these sketches to indicate extent of injection sites.

DISCUSSION

In the present study, the PHA-L method was used to investigate projections of the inferior olivary complex to the cerebellum. Dense nerve terminal plexuses were observed in the cerebellar nuclei, supporting the proposal that collaterals of the climbing fibers innervate these nuclei.

Methodological considerations

The question of climbing fiber input to the cerebellar nuclei has been addressed by several neuroanatomical techniques. A number of authors have used retrograde tracing techniques (Beitz, '76; Eller and Chan-Palay, '76; Kitai et al., '77; Dietrichs and Walberg, '85, '86, '87; Dietrichs et al., '85). But because nonterminal olivocerebellar axons pass immediately around and through the deep nuclei, retrograde tracing cannot be considered a method of choice to determine if olivary axons terminate in these nuclei. Other

investigators used anterograde tracing with radioactively labelled amino acids; but, in the light microscope, it is difficult to determine if autoradiographic accumulations of silver grains correspond to terminals or fibers of passage. This pre-

Fig. 13.   Schematic representation of an experiment with a PHA-L injection centered on the rostral MAO, but also involving the ventral lamella of PO. Injection site represented by diagrams (lower right); dense hatching represents the center of injection, which showed intense immunoreactivity; less intensely labelled regions are indicated by stippling. The cerebellum was sectioned sagittally, and representative sections are shown from lateral (1) to medial (5). Labelled axons are indicated as wavy lines and terminal fibers as dots. Note the many labelled olivocerebellar axons arriving via the restiform body (2) continuing above or through the cerebellar nuclei and the bundles of fibers running through the folial white matter. Climbing fiber terminals appear in several cortical regions. Plexuses of terminal fibers appear in the NIP and sparsely in the LCN.
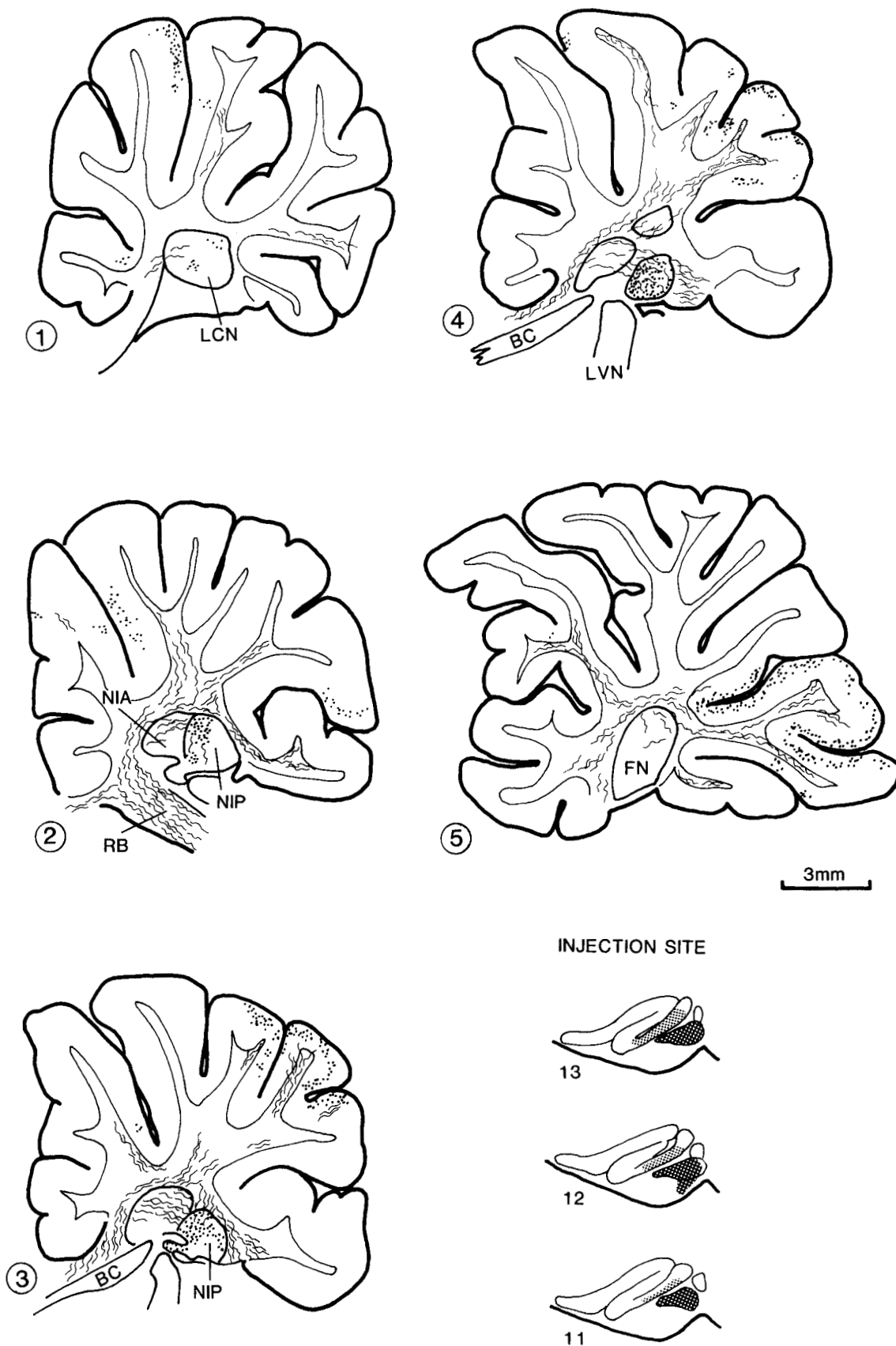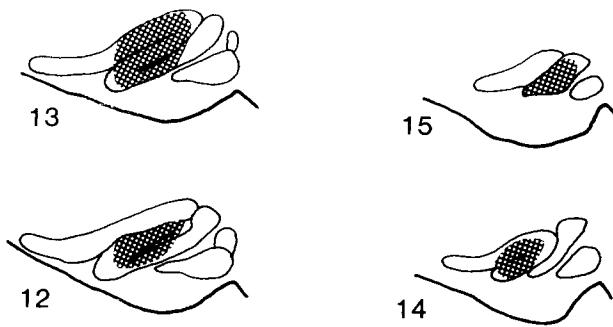
Figure 13

Fig. 14. Schematic representation of an experiment with an injection involving rostral PO and DAO (same as in Fig. 6). On the frontal cerebellar section, labelled fibers are seen in the restiform body and cerebellar white matter. Sagittally organized zones of climbing fiber ter-

minals appear in crus I and paraflocculus. A dense plexus of terminals appears in a sector of the LCN, and the NIA demonstrates a less dense innervation. Symbols as in Figure 13.
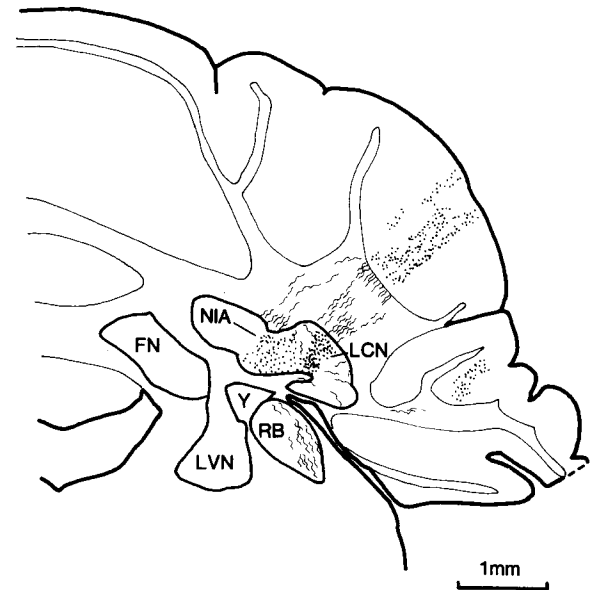
sumably explains why some authors have interpreted their results in favour (Groenewegen and Voogd, '77; Courville and Faraco-Cantin, '78; Groenewegen et al., '79) and others against (Courville, '75) the existence of olivonuclear innervation. Electron microscopic investigation of autoradiographic labelling can provide unambiguous evidence, and using this technique van der Want and Voogd ('87) demonstrated the existence olivary terminals forming axodendritic synapses in the FN of the cat.

The method of PHA-L tracing has advantages over other tracing methods, as it allows visualization of morphological characteristics distinguishing nonterminal and terminal axons at the light microscopical level. The methodological observations of the present study agree with previous descriptions of the PHA-L technique (Gerfen and Sawchenko, '84; Wouterlood and Groenewegen, '85), but some new aspects of tracing pathways with this lectin were noted. Suggestive evidence for transneuronal PHA-L labelling was noted in Purkinje cells contacted by intensely labelled climbing fiber terminals. This labelling appeared as a weak cytoplasmic outlining of the contacted Purkinje cell and could not be mistaken for anterograde axonal labelling. It should be underlined that a climbing fiber establishes numerous powerful synaptic contacts with the Purkinje cell (Eccles et al., '67; Palay and Chan-Palay, '74). If small amounts of lectin are released by each bouton, transsynaptic transfer of the tracer could be more easily observed in the climbing fiber system than in many other neuronal connections. Another unexpected example of transcellular transfer of PHA-L was the observation of labelled glia amidst bundles of intensely labelled axons.

Retrograde labelling with PHA-L has been reported previously (Kita and Kitai, '87) and was frequently noted in our material over distances of several hundred micrometers to a millimeter. The most informative observations were made

in cases in which labelled olivary neurons appeared contralaterally to the injection site. These cells occurred in olivary regions known to project through the center of the iontophoretic injection site, and it may therefore be proposed that lesioning of passing fibers may be necessary for this retrograde labelling.

Terminals in cerebellar nuclei

In the present PHA-L study, labelled olivocerebellar axons were visualized in detail. Olivary axons reaching the deep cerebellar white matter via the contralateral restiform body ran closely around and through the cerebellar nuclei. In circumscribed regions of the deep nuclei, plexuses of labelled thin fibers of nerve terminal character appeared and displayed morphological characteristics that set them apart from the thicker nonterminal olivary axons. The intervaricose segments of these fine fibers measured 0.4–0.5 μm in diameter and were more difficult to visualize than the larger varicose boutons, which measured 1–1.4 μm.

These terminal fibers obviously originated from olivary axons, which converged on the regions of nerve terminal plexuses; moreover, the thicker nonterminal olivary axons could be seen to give off thin collaterals to the innervated areas. The distinct topography of nuclear innervation was reproducibly related to the area of the olive that had been injected with PHA-L. Finally, after efficient pretreatment with 3-AP, PHA-L injections in the region of the lesioned olive failed to label terminal fiber plexuses in the deep nuclei, as well as other features of the olivocerebellar climbing fiber system.

Taken together, these aspects provide strong evidence for the olivary origin of the observed plexuses of fine terminals innervating the deep nuclei. Electron microscopic analysis of these labelled plexuses is necessary to prove the synaptic nature of the varicosities and to identify their synaptic tar-
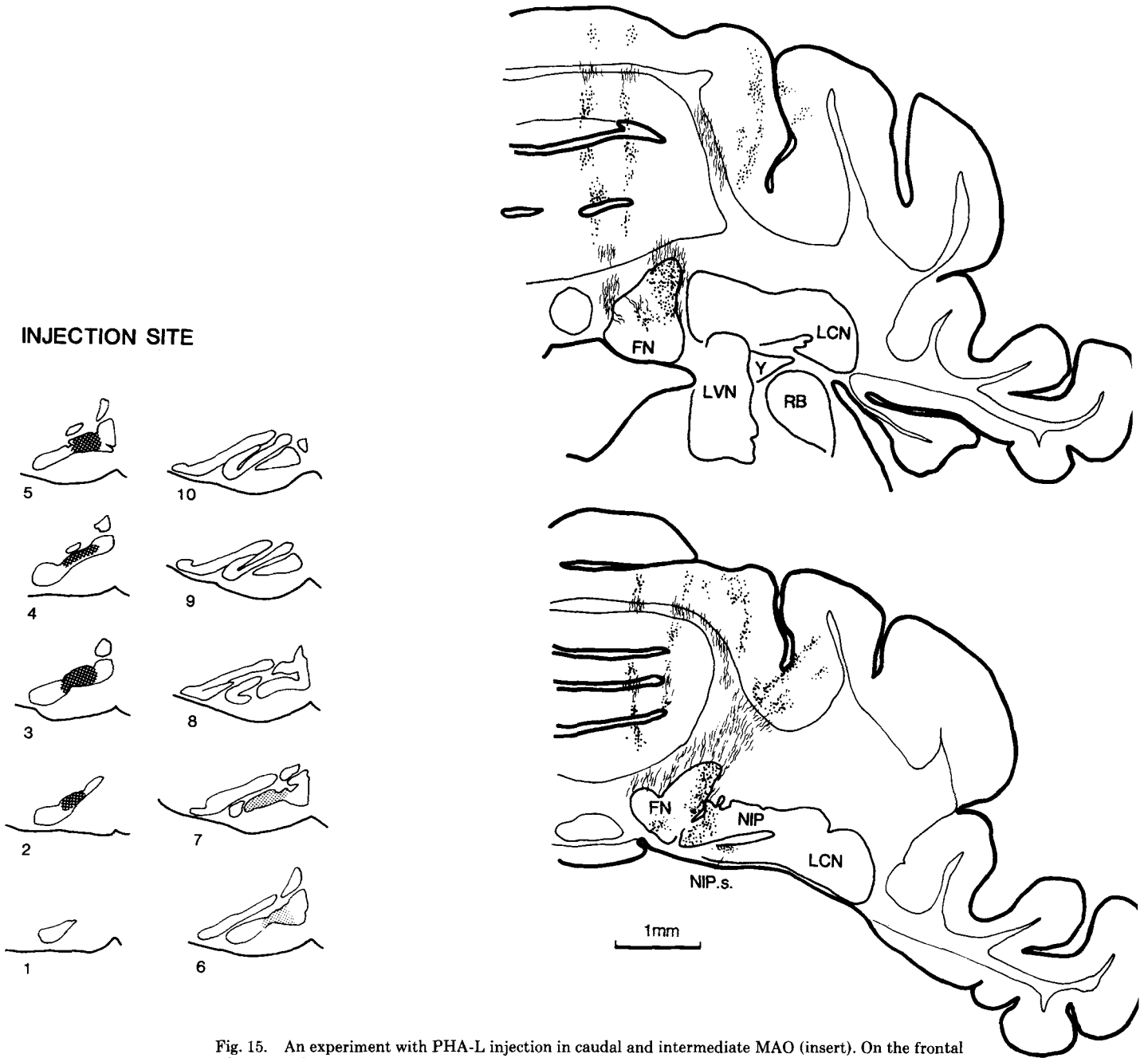
INJECTION SITE

Fig. 15. An experiment with PHA-L injection in caudal and intermediate MAO (insert). On the frontal cerebellar sections, terminal innervation appears in regions of the FN and medially in the NIP. Bundles of labelled axons run toward zones of climbing fiber termination in the vermal and intermediate parts of cortex. Symbols as in Figure 13.

gets, but preliminary experiments have shown that these weakly labelled terminal fibers are difficult to identify on the ultrastructural level (van der Want, unpublished). In basal ganglia, electron microscopic studies have shown that similar PHA-L-labelled varicose fibers correspond to axon terminals engaging in synaptic junctions (Wouterlood and Groenewegen, '85; Kita and Kitai, '87). Thus, even without complete ultrastructural information on the PHA-L labelled fiber plexuses in the cerebellar nuclei, it seems a reasonable assumption that these fibers form a synaptic innervation (van der Want and Voogd, '87) and that they are the

morphological correlate to the climbing fiber-evoked epsp's that precede the Purkinje cell evoked ipsp's in the deep cerebellar nuclei when stimulating climbing fiber pathways (Andersson and Oscarsson, 1978).

The observation that thicker olivary axons sent collaterals to these plexuses is in line with the idea that the olivonuclear innervation represents collaterals of cortical climbing fibers (Eccles et al., '74; Andersson and Oscarsson, '78; Wiklund et al., '84), but our PHA-L data do not exclude the possibility that some olivonuclear fibers do not terminate in the cerebellar cortex. Evidence for the collateral origin of the

olivonuclear innervation has previously been obtained by retrograde D-[³H]aspartate labelling; cortical injections of this tracer resulted in collateral labelling in cortex as well as dense terminal labelling in the deep nuclei (Wiklund et al., '84).

The anatomical discussion on the existence of climbing fiber terminals in the deep nuclei has often become a question of whether they are "very few" or "many enough" to have a physiological role (Eccles et al., '67). Therefore, we decided to count the number of PHA-L-labelled boutons in some areas of dense olivonuclear innervation. In the FN, interposed nuclei, and main parts of LCN, these estimates arrived at terminal densities of 1.7–4.3 million boutons per mm³, which indicates that the olivocerebellar terminals represent a considerable input to the deep nuclear neuropil. The parvocellular portion of LCN, which receives innervation from medial parts of caudal MAO, demonstrated higher densities of 15–20 million varicosities per mm³*.

These estimates can be compared with the quantitative study of synapses in the cerebellar nuclei of the cat by Palkovits et al. ('77). The total density of synaptic terminals in the different nuclei calculated by these authors was 27.8–42.3 millions/mm³ (calculated from their Table 4), and they estimated 62% to represent Purkinje cell synapses. Chan-Palay ('73, '77) used ultrastructural similarities with cortical climbing fibers to identify presumed climbing fiber collaterals in the LCN and estimated that these comprised 5–6% of the total number of terminals. This estimate seems well compatible with the results of the present study.

Olivonuclear topography; comparison with other tracing data

The topographical organization of the olivonuclear projections observed in the present study agreed with the organization reported by Groenewegen and Voogd ('77) and Groenewegen et al. ('79) in their autoradiographic tracing studies in the cat. Thus, caudal MAO was found to project to FN, rostral MAO to NIP, rostral DAO to NIA, and PO to LCN. Our material did not include any injection into the caudal DAO areas, which are believed to project to the dorsal parts of Deiters' nucleus (Groenewegen and Voogd, '77; Wiklund et al., '84).

The olivonuclear topography has also been studied by Dietrichs and collaborators in a series of investigations using retrograde tracing methods (Dietrichs et al., '85; Dietrichs and Walberg, '85, '86). Most of their results are in agreement with the present study, but a notable discrepancy involves the olivary projections to the interposed nuclei. It remains a possibility that species differences between the cat and rat can explain the difference, but the presence of numerous labelled cells in both accessory olives after WGA-HRP implantations into NIA in the study of Dietrichs and Walberg ('86) would be in accordance with the presence of both terminating fibers (from DAO) and passing fibers (from MAO) in this nucleus. This explanation is supported by the abscence or scarcety of retrogradely labelled cells in the DAO after WGA-HRP implantations in NIP.

Interestingly, the topography of the olivonuclear projections revealed in the present and other investigations

(Groenewegen and Voogd, '77; Groenewegen et al., '79; Dietrichs et al., '85; Dietrichs and Walberg, '85), the olivocerebellar (Groenewegen and Voogd, '77; Groenewegen et al., '79; Brodal and Kawamura, '80; Azizi and Woodward, '87; Bernard, '87) and corticonuclear Purkinje cell projection (Dietrichs and Walberg, '79, '80; Dietrichs, '81a,b, '83; Trott and Armstrong, '87a,b) suggest that a "closed circuit" is created; the climbing fibers terminating on the Purkinje cells projecting to the cerebellar nulear region receiving collaterals from the same olivary axons (Voogd, '82; Dietrichs et al., '85).

CONCLUSIONS AND FUNCTIONAL IMPLICATIONS

This study demonstrated a topographically organized olivary input to the cerebellar nuclei. At least part of this innervation consists of collaterals of olivary axons terminating in the cerebellar cortex as climbing fibers.

Considerable efforts are being made to understand the functional principles of cerebellar circuitry. Functional models (Marr, '69; Albus, '71) have suggested that the climbing fibers influence the Purkinje cell responsiveness to parallel fibers, and experimental results have indicated that conjunctive climbing fiber activity leads to a powerful and lasting decrease in parallel fiber responsiveness (Ito et al., '82; Ekerot and Kano, '85). The existence of an abundant climbing fiber collateral innervation in the deep nuclei has to be integrated into new models of cerebellar function. It can be questioned if the nuclear climbing fiber collaterals have a similar role in modulating the cerebellar efferent responses to incoming information.

ACKNOWLEDGMENTS

LITERATURE CITED

Albus, J.S. (1971) A theory of cerebellar function. Math. Sci. 10:25–61.

Andersson, G., and O. Oscarsson (1978) Projections to lateral vestibular nucleus from cerebellar climbing fibre zones. Exp. Brain Res. 32:549–564.

Angaut, P. (1975) Synaptology of brain stem afferents to the cerebellar nuclei in the cat. An experimental electron microscopic study. (abstract) Exp. Brain Res. (Suppl.) 23:12.

Armstrong, D.M., R.J. Harvey, and R.F. Schild (1973a) Cerebello-cerebellar responses mediated via climbing fibres. Exp. Brain Res. 18:19–39.

Armstrong, D.M., R.J. Harvey, and R.F. Schild (1973b) The spatial organization of climbing fibre branching in the cat cerebellum. Exp. Brain Res. 18:40–58.

Azizi, S.A., and D.J. Woodward (1987) Inferior olivary nuclear complex of the rat: morphology and comments on the principle of organization within the olivocerebellar system. J. Comp. Neurol. 263:467–484.

Balaban, C.D. (1985) Central neurotoxic effects of intraperitoneally administered 3-acetylpyridine, harmaline and niacinamide in Sprague-Dawley and Long Evans rats: A critical review of central 3-acetylpyridine neurotoxicity. Brain Res. Rev. 9:21–42.

Beitz, A.J. (1976) The topographical organization of the olivo-dentate and dentato-olivary pathways in the cat. Brain Res. 115:311–317.

Bernard, J.F. (1987) Topographical organization of olivocerebellar and corticonuclear connections in the rat. An WGA-HRP study: I. Lobules IX,X and the flocculus. J. Comp. Neurol. 263:241–258.

---

*These estimates, made on thick (30 μm) sections, should be regarded as approximative. Counting terminal density on thinner, e.g., plastic embedded sections, would have represented a more accurate method.

Brodal, A. (1940) Experimentelle Untersuchungen über die olivo-cerebellare Lokalisation. Z. Gesamte Neurol. Psychiat. *169*:1–153.

Brodal, A., and K. Kawamura (1980) Olivocerebellar projection: A review. Adv. Anat. Embryol. Cell Biol. *64*:1–140.

Brodal, A., F. Walberg, K.J. Berkley, and A. Pelt (1980) Anatomical demonstration of branching olivocerebellar fibres by means of a double retrograde labelling technique. Neuroscience *5*:2193–2202.

Cajal, S.R.y. (1911) Histologie du Système Nerveux de l'Homme et des Vertébres. Vol. II. Paris: Maloine.

Campbell, N.C., and D.M. Armstrong (1983a) The olivocerebellar projection in the rat: an autoradiographic study. Brain Res. *275*:215–233.

Campbell, N.C., and D.M. Armstrong (1983b) Topographical localization in the olivocerebellar projection in the rat: An autoradiographic study. Brain Res. *275*:235–249.

Chan-Palay, V. (1973) On the identification of afferent axon terminals in the nucleus lateralis of the cerebellum. An electron microscope study. Z. Anat. Entwickl.-Gesch. *142*:149–186.

Chan-Palay, V. (1977) Cerebellar Dentate Nucleus: Organization, Cytology and Transmitters. Berlin: Springer.

Courville, J. (1975) Distribution of olivocerebellar fibers demonstrated by a radioautographic tracing method. Brain Res. *95*:253–263.

Courville, J., and F. Faraco-Cantin (1978) On the origin of the climbing fibers of the cerebellum. An experimental study in the cat with an autoradiographic tracing method. Neuroscience *3*:797–809.

Desclin, J.C. (1974) Histological evidence supporting the inferior olive as the major source of cerebellar climbing fibers in the rat. Brain Res. *77*:365–384.

Desclin, J.C., and F. Colin (1980) The olivocerebellar system. II. Some ultrastructural correlates of inferior olive destruction in the rat. Brain Res. *187*:29–46.

Desclin, J.C., and J. Escubi (1974) Effects of 3-acetylpyridine on the central nervous system of the rat, as demonstrated by silver methods. Brain Res. *77*:349–364.

Dietrichs, E. (1981a) The cerebellar corticonuclear and nucleocortical projections in the cat as studied with anterograde and retrograde transport of horseradish peroxidase. III. The anterior lobe. Anat. Embryol. *162*:223–247.

Dietrichs, E. (1981b) The cerebellar corticonuclear and nucleocortical projections in the cat as studied with anterograde and retrograde transport of horseradish peroxidase. IV. The paraflocculus. Exp. Brain Res. *44*:235–242.

Dietrichs, E. (1983) The cerebellar corticonuclear and nucleocortical projections in the cat as studied with anterograde and retrograde transport of horseradish peroxidase. V. The posterior lobe vermis and the flocculonodular lobe. Anat. Embryol. *167*:449–462.

Dietrichs, E., and F. Walberg (1979) The cerebellar corticonuclear and nucleocortical projections in the cat as studied with anterograde and retrograde transport of horseradish peroxidase. I. The paramedian lobule. Anat. Embryol. *158*:13–39.

Dietrichs, E., and F. Walberg (1980) The cerebellar corticonuclear and nucleocortical projections in the cat as studied with anterograde and retrograde horseradish peroxidase. II. Lobus simplex, crus I and crus II. Anat. Embryol. *161*:83–103.

Dietrichs, E., F. Walberg, and T. Nordby (1985) The cerebellar nucleo-olivary and olivo-cerebellar nuclear projections in the cat as studied with anterograde and retrograde transport in the same animal after implantation of crystalline WGA-HRP. I. The dentate nucleus. Neurosci. Res. *3*:52–70.

Dietrichs, E., and F. Walberg (1985) The cerebellar nucleo-olivary and olivocerebellar nuclear projections in the cat as studied with anterograde and retrograde transport in the same animal after implantation of crystalline WGA-HRP. II. The fastigial nucleus. Anat. Embryol. *173*:253–261.

Dietrichs, E., and F. Walberg (1986) The cerebellar nucleo-olivary and olivocerebellar nuclear projections in the cat as studied with anterograde and retrograde transport in the same animal after implantation of crystalline WGA-HRP. III. The interposed nuclei. Brain Res. *373*:373–383.

Dietrichs, E., and F. Walberg (1987) Cerebellar nuclear afferents—where do they originate? A re-evaluation of the projections from some lower brain stem nuclei. Anat. Embryol. *177*:165–172.

Eccles, J.C., M. Ito, and J. Szentágothai (1967) The Cerebellum as a Neuronal Machine. Berlin: Springer.

Eccles, J.C., N.H. Sabah, and H. Táboriková (1974) The pathways responsible for excitation and inhibition of fastigial neurons. Exp. Brain Res. *19*:78–99.

Eisenman, L.M. (1984) Organization of olivocerebellar projection to the uvula in the rat. Brain Behav. Evol. *24*:1–12.

Eller, T., and V. Chan-Palay (1976) Afferents to the cerebellar lateral nucleus. Evidence from retrograde transport of horseradish peroxidase after pressure injections through micropipettes. J. Comp. Neurol. *166*:285–302.

Ekerot, C.-F., and M. Kano (1985) Long term depression of parallel fibre synapses following stimulation of climbing fibres. Brain Res. *342*:357–360.

Gerfen, C.R., and P.F. Sawchenko (1984) An anterograde neuroanatomical tracing method that shows detailed morphology of neurons, their axons and terminals: immunohistochemical localization of an axonally transported plant lectin, Phaseolus vulgaris-leucoagglutinin (PHA-L). Brain Res. *290*:219–238.

Gerrits, N.M., and J. Voogd (1987) The projection of the nucleus reticularis tegmenti pontis and adjacent regions of the pontine nuclei to the central cerebellar nuclei in the cat. J. Comp. Neurol. *258*:52–69.

Groenewegen, H.J., and C.A. Van Dijk (1984) Efferent connections of the dorsal tegmental region in the rat, studied by means of anterograde transport of the lectin Phaseolus vulgaris-leucoagglutinin (PHA-L). Brain Res. *304*:367–371.

Groenewegen, H.J., and J. Voogd (1977) The parasagittal zonation within the olivocerebellar projection. I. Climbing fiber distribution in the vermis of the cat cerebellum. J. Comp. Neurol. *174*:417–488.

Groenewegen, H.J., J. Voogd, and S.L. Freedman (1979) The parasagittal zonation within the olivocerebellar projection. II. Climbing fiber distribution in the intermediate and hemispheric parts of cat cerebellum. J. Comp. Neurol. *183*:551–602.

Gwyn, D.G., G.P. Nicholson, and B.A. Flumerfelt (1977) The inferior olivary nucleus of the rat: A light and electron microscopic study. J. Comp. Neurol. *174*:489–520.

Ikeda, M., and M. Matsushita (1973) Electron microscopic observations on the spinal projections to the cerebellar nuclei in the cat and rabbit. Experientia *29*:1280–1282.

Ito, M., M. Sakurai, and P. Tongroach (1982) Cerebellar climbing fibre induced depression of both mossy fibre responsiveness and glutamate sensitivity of cerebellar Purkinje cells. J. Physiol. (Lond.) *324*:113–134.

Itoh, K., A. Konishi, S. Nomura, N. Mizuno, Y. Nakamura, and T. Sugimoto (1979) Application of coupled oxidase reaction to electron microscopic demonstration of horseradish peroxidase: Cobalt-glucose oxidase method. Brain Res. *175*:341–346.

Kita, H., and S.T. Kitai (1987) Efferent projections of the subthalamic nucleus in the rat: Light and electron microscopic analysis with the PHA-L method. J. Comp. Neurol. *260*:435–452.

Kitai, S.T., R.A. McCrea, R.J. Preston, and G.A. Bishop (1977) Electrophysiological and horseradish peroxidase studies of precerebellar afferents to the nucleus interpositus anterior. I. Climbing fiber system. Brain Res. *122*:197–214.

Korneliussen, H.K. (1968) On the morphology and the subdivision of the cerebellar nuclei of the rat. J. Hirnforsch. *10*:109–122.

Künzle, H. (1975) Autoradiographic tracing of the cerebellar projections from the lateral reticular nucleus in the cat. Exp. Brain Res. *22*:255–266.

Llinás, R., K. Walton, D.E. Hillman, and C. Sotelo (1975) Inferior olive: its role in motor learning. Science *190*:1230–1231.

Marr, D. (1969) A theory of cerebellar cortex. J. Physiol. (Lond.) *202*:437–470.

Matsushita, M., and M. Ikeda (1970) Olivary projections to the cerebellar nuclei in the cat. Exp. Brain Res. *10*:488–500.

Palay, S.L., and V. Chan-Palay (1974) Cerebellar Cortex. Cytology and Organization. Berlin: Springer Verlag.

Palkovits, M., E. Mezey, J. Hamori, and J. Szentágothai (1977) Quantitative histological analysis of the cerebellar nuclei in the cat. I. Numerical data on cells and on synapses. Exp. Brain Res. *28*:189–209.

Rosina, A., and L. Provini (1983) Somatotopy of climbing fiber branching to the cerebellar cortex in cat. Brain Res. *289*:45–63.

Russchen, F.T., H. Groenewegen, and J. Voogd (1976) Reticulocerebellar fibers in the cat. An autoradiographic study. Acta Morphol. Neerl. Scand. *14*:245–246.

Sotelo, C., D.E. Hillman, A.J. Zamora, and R. Llinás (1975) Climbing fiber deafferentation: its action on Purkinje cell dendritic spines. Brain Res. *98*:574–581.

Trott, J., and D.M. Armstrong (1987a) The cerebellar cortico-nuclear projection from lobule V b/c of the cat anterior lobe: A combined electrophysiological and autoradiographic study. I. Projections from the intermediate region. Exp. Brain Res. *66*:318–338.

Trott, J., and D.M. Armstrong (1987b) The cerebellar cortico-nuclear projection from lobule V b/c of the cat anterior lobe: A combined electro-

physiological and autoradiographic study. II. Projections from the vermis. Exp. Brain Res. *68*:339–354.

Van der Want, J.J.L., N.M. Gerrits, and J. Voogd (1987) Autoradiography of mossy fiber terminals in the fastigial nucleus of the cat. J. Comp. Neurol. *258*:70–80.

Van der Want, J.J.L., and J. Voogd (1987) Ultrastructural identification and localisation of climbing fiber terminals in the fastigial nucleus of the cat. J. Comp. Neurol. *258*:81–90.

Van der Want, J.J.L., M. Guegan, L. Wiklund, C. Buisseret-Delmas, T. Ruigrok, and J. Voogd (1988) Climbing fiber collateral innervation of the central cerebellar nuclei studied with anterograde Phaseolus vulgaris-leucoagglutinin (PHA-L) labelling. In P. Strata (ed): The Olivocerebellar System in Motor Control. Exp. Brain Res., Series 17. Berlin: Springer-Verlag pp. 82–85.

Voogd, J. (1964) The Cerebellum of the Cat. Structure and Fiber Connections. Thesis. Assen: Van Gorcum.

Voogd, J. (1982) The olivocerebellar projection in the cat. In S.L. Palay and

V. Chan-Palay (eds): The Cerebellum New Vistas. Exp. Brain Res. [Suppl. 6]: pp. 134–161.

Voogd, J., and F. Bigaré (1980) Topographical distribution of olivary and corticonuclear fibers in the cerebellum: A review. In J. Courville et al. (eds): The Inferior Olivary Nucleus. Anatomy and Physiology. New York: Raven Press, pp. 207–277.

Voogd, J., N.M. Gerrits, and E. Marani (1985) Cerebellum. In G. Paxinos (ed): The Rat Nervous System, Vol. 2, London: Academic Press, pp. 251–291.

Wiklund, L., G. Toggenburger, and M. Cuénod (1984) Selective retrograde labelling of the rat olivocerebellar climbing fiber system with D-[^{3}H] aspartate. Neuroscience *13*:441–468.

Wouterlood, F.G., and H.J. Groenewegen (1985) Neuroanatomical tracing by use of Phaseolus vulgaris-leucoagglutinin (PHA-L): Electron microscopy of PHA-L-filled neuronal somata, dendrites, axons and axon terminals. Brain Res. *326*:188–191.